A revised parameterization for gaseous dry deposition in air-quality models

L. Zhang, J. R. Brook, R. Vet

To cite this version:

L. Zhang, J. R. Brook, R. Vet. A revised parameterization for gaseous dry deposition in air-quality models. Atmospheric Chemistry and Physics Discussions, European Geosciences Union, 2003, 3 (2), pp.1777-1804. <hal-00301000>

HAL Id: hal-00301000

https://hal.archives-ouvertes.fr/hal-00301000

Submitted on 28 Mar 2003

HAL is a multi-disciplinary open access archive for the deposit and dissemination of scientific research documents, whether they are published or not. The documents may come from teaching and research institutions in France or abroad, or from public or private research centers.

L'archive ouverte pluridisciplinaire **HAL**, est destinée au dépôt et à la diffusion de documents scientifiques de niveau recherche, publiés ou non, émanant des établissements d'enseignement et de recherche français ou étrangers, des laboratoires publics ou privés.

Atmos. Chem. Phys. Discuss., 3, 1777–1804, 2003
www.atmos-chem-phys.org/acpd/3/1777/
© European Geosciences Union 2003

Atmospheric
Chemistry
and Physics
Discussions

A revised parameterization for gaseous dry deposition in air-quality models

L. Zhang, J. R. Brook, and R. Vet

Meteorological Service of Canada, 4905 Dufferin Street, Toronto, Ontario, M3H 5T4, Canada

Received: 11 March 2003 – Accepted: 18 March 2003 – Published: 28 March 2003

Correspondence to: L. Zhang (leiming.zhang@ec.gc.ca)

Abstract

A parameterization scheme for calculating gaseous dry deposition velocities in air-quality models is revised based on recent study results on non-stomatal uptake of O_3 and SO_2 over 5 different vegetation types. Non-stomatal resistance, which includes in-canopy aerodynamic resistance, soil resistance and cuticle resistance, for SO_2 and O_3 is parameterized as a function of friction velocity, relative humidity, leaf area index, and canopy wetness. Non- stomatal resistance for all other species is scaled to those of SO_2 and O_3 based on their chemical and physical characteristics. Stomatal resistance is calculated using a leaf-stomatal-resistance model for all gaseous species of interest. The improvements in the present model compared to its earlier version include a newly developed non-stomatal resistance formulation, a realistic treatment of cuticle and ground resistance in winter and the handling of seasonally-dependent input parameters. Model evaluation shows that the revised parameterization can provide more realistic deposition velocities for both O_3 and SO_2, especially for wet canopies. Example model output shows that the parameterization provides reasonable estimates of dry deposition velocities for different gaseous species, land types and diurnal and seasonal variations. Maximum deposition velocities from model output are close to reported measurement values for different land types. The current parameterization can be easily adopted into different air-quality models that require inclusion of dry deposition processes.

1. Introduction

Dry deposition is an important process that requires treatment in regional air-quality models. Wesely (1989) developed a parameterization scheme for estimating gaseous dry deposition velocities, which has been widely used in a number of models (RADM, Chang et al., 1987; STEM, Carmichael et al., 1991; URM, Harley et al., 1993; CMAQ, Byun and Ching, 1999). Similar dry deposition models have been developed for air-

© EGU 2003

quality models by Padro et al. (1991), Scire (1991), Pleim and Xiu (1995) and Zhang et al. (2002a). Dry deposition models have also been used in estimating total acid deposition. For this purpose, some single layer (usually called big-leaf) and multi-layer dry deposition models have also been developed (Erisman et al., 1994; Meyers et al., 1998; Brook et al., 1999a; Smith et al., 2000). A review of available dry deposition models was recently reported by Wesely and Hicks (2000).

Most existing dry deposition models utilize the multiple resistance analogy approach when parameterizing the deposition velocity to vegetation and other surfaces. In this approach, the canopy resistance is usually separated into stomatal and non-stomatal portions. While the overall deposition flux is the major concern of most air-quality models, it can be important to separate the stomatal uptake of pollutants from the overall deposition for some applications (e.g. O_3 dose to agricultural crops). Separating stomatal and non-stomatal uptake also allows us to model the diurnal variations of dry deposition more accurately, especially since stomatal uptake only occurs during the daytime for most canopy species, during which time it dominates over non-stomatal uptake. There are many different approaches for stomatal resistance calculations ranging from simple parameterizations as functions of solar radiation and/or time of day (Wesely, 1989; Padro et al., 1991), one- or two-big-leaf approaches (Jarvis, 1976; Hicks et al., 1987; Zhang et al., 2002a), to a multi-layer leaf-resistance model (Baldocchi et al., 1987). For non-stomatal resistance, a constant is usually chosen for a particular season or land type, thereby excluding the effects of meteorology. However, many recent measurements have shown that non-stomatal resistance is also affected by meteorological conditions, e.g. friction velocity ($u*$), relative humidity (RH) and canopy wetness, in addition to biological factors, e.g. canopy type, leaf area index (LAI) and growing period. For example, measurements over several different canopies (forests, maize) in France (Lamaud et al., 2002; Laville et al., 2002; Lopez et al., 2002) all show that the non-stomatal uptake of O_3 (e.g. the nighttime deposition) is controlled by the friction velocity. Zhang et al. (2002b) analyzed O_3 deposition flux data from measurements taken over five different canopies (mixed forest, deciduous forest, corn, soybean and pasture) in the eastern USA (Finkelstein et al., 2000; Meyers et al., 1998) and found that the non-stomatal resistance is affected by $u*$, RH, LAI, canopy wetness and possibly other factors that were not measured. Based on the data from these five sites, Zhang et al. (2002b) proposed a set of parameterizations for the non-stomatal resistance of O_3. Zhang et al. (2003) further evaluated this set of parameterization, with adjustments to some parameters, using SO_2 flux data measured at the same five canopies and obtained very good agreement between model results and measurements.

Zhang et al. (2002a) developed a parameterization scheme (a big-leaf model), similar to the approach used in Wesely (1989), for calculating dry deposition velocities for 30 gaseous species that are usually considered in air-quality models. Only seasonally adjusted values are used for non-stomatal resistance and meteorological effects are not considered. The purpose of the present study is to revise the parameterization scheme developed by Zhang et al. (2002a) by adopting the newly developed non-stomatal resistance parameterization presented in Zhang et al. (2002b, 2003). Other improvements include more realistic treatment of cuticle and ground resistance in winter and the handling of seasonally-dependent input parameters. The land use categories (LUC) used in Zhang et al. (2002a) are based, with some modifications, on BATS (Biosphere Atmosphere Transfer Scheme, Dickinson, 1986), a widely-used scheme in North America. In the present study, the surface scheme of GEM (Global Environmental Multi-scale model, Coté et al., 1997), Canada's operational weather forecast model, is used. This is because GEM is, or will be, used as the meteorological driver for many Canadian air-quality models, e.g. AURAMS (Moran et al., 1998) and CHRONOS (Pudykiewicz et al., 1997). Furthermore, this LUC scheme is based on BATS with an extra 6 LUCs. Choosing this 26-category scheme will also benefit air-quality models developed elsewhere.

The next section describes in detail the model equations. Two important input parameters (LAI and roughness length z_0) are given in Sect. 3. Comparison of model results with single site measurements of O_3 and SO_2 dry deposition velocity and example model output are given in Sect. 4.

2. Model description

The scheme for the revised model is shown in Fig. 1. The primary resistances to pollutant uptake are the aerodynamic resistance (R_a), the quasi-laminar sublayer resistance (R_b) above the canopy, and the overall canopy resistance (R_c). R_c can be separated into two parallel paths; one is stomatal resistance (R_{st}) with its associated mesophyll resistance (R_m), and the other is non-stomatal resistance (R_{ns}). R_{ns} can be further decomposed into resistance to soil uptake, which includes in-canopy aerodynamic resistance (R_{ac}) and the subsequent soil resistance (R_g), as well as resistance to cuticle uptake (R_{cut}). Note that R_{cut} here is slightly different from that defined in traditional big-leaf models in that it also considers the aerodynamic and quasi-laminar resistances to individual leaves. This is done by parameterizing R_{cut} as a function of friction velocity, similar to the concept of overall cuticle uptake considered in a multi-layer model framework (e.g. Baldocchi, 1988).

Based on the above discussion, the dry deposition velocity, V_d, is defined as:

$$V_d = \frac{1}{R_a + R_b + R_c}, \tag{1}$$

where expressions for R_a and R_b can be computed as in many earlier dry deposition studies (e.g. Padro, 1996). The uncertainties in R_a and R_b from the different models are small. In the present study, only R_c is discussed. R_c is parameterized as:

$$\frac{1}{R_c} = \frac{1 - W_{st}}{R_{st} + R_m} + \frac{1}{R_{ns}} \tag{2}$$

$$\frac{1}{R_{ns}} = \frac{1}{R_{ac} + R_g} + \frac{1}{R_{cut}}, \tag{3}$$

where W_{st} is the fraction of stomatal blocking under wet conditions. R_{st} is calculated using a sunlit/shade (two-big-leaf) stomatal resistance approach. R_m is treated as dependent only on the chemical species and the values for some common species

© EGU 2003

considered in air-quality models can be found in Zhang et al. (2002a). Note that Eqs. (2) and (3) are for surfaces with canopies. For surfaces without canopies (e.g. water, ice, desert), R_{st}, R_m, R_{ac} and R_{cut} are not applicable. For the convenience of using the same equations for all LUCs, we define R_g as resistances to any surfaces (soil, ice, snow, water), (more discussion below). Thus, for surfaces without canopy, a value of 0 is given to R_{ac} and a very large value (i.e. $10^{25}\,\mathrm{s\,m^{-1}}$) should be used for R_{st}, R_m and R_{cut}.

R_{ac} is not species-dependent while R_g and R_{cut} are. R_g and R_{cut} are calculated for SO_2 and O_3 and then scaled for other gaseous species based on the equation:

$$\frac{1}{R_x(i)} = \frac{\alpha(i)}{R_x(\mathrm{SO_2})} + \frac{\beta(i)}{R_x(\mathrm{O_c})}, \tag{4}$$

where R_x represents non-stomatal resistance components (i.e. R_{cut} and R_g) and i represents the particular gaseous species. Parameters α and β are two scaling factors and are functions of the chemical species. Scaling parameters for a total of 30 species has been presented in Table 1 of Zhang et al. (2002a). The details of each term in Eqs. (2)–(4) are discussed below.

$\mathbf{W_{st}}$: Zhang et al. (2002b), using O_3 flux data from five sites in eastern North America, found that W_{st} is not important under most wet conditions because of weak solar radiation (SR), which leads to large R_{st}. However, there are some exceptions such as morning dew and sunshine immediately after rain when the stomata can be blocked but solar radiation is strong. Under these conditions, W_{st} should be considered. Thus, the following equation is suggested for wet canopies (for dry canopies, W_{st} always equals to 0):

$$W_{st} = \begin{cases} 0, & SR \le 200\,\mathrm{W\,m^{-2}} \\ (SR-200)/800, & 200 < SR \le 600\,\mathrm{W\,m^{-2}} \\ 0.5, & SR > 600\,\mathrm{W\,m^{-2}} \end{cases} \tag{5}$$

W_{st} is given a value other than 0 only when solar radiation is relatively strong (>200 W m^{-2}) and the canopy is wet. If rain or dew occurs, the canopy is treated as wet. Occurrence of dew can be defined based on particular meteorological conditions, e.g. RH, u_* and cloud cover (Janssen and Romer, 1991) as adopted in Brook et al. (1999a).

R

$\mathbf{R_{st}}$: A sunlit/shade (two-big-leaf) stomatal resistance sub-model described in Zhang et al. (2002a) is used for calculating R_{st} for all gaseous species. R_{st} is calculated as:

$$R_{st} = 1/\left[G_s(PAR)f(T)f(D)f(\Psi)(D_i/D_v)\right], \tag{6}$$

where $G_s(PAR)$ is the unstressed leaf stomatal conductance, a function of photosynthetically active radiation (PAR). Calculation of $G_s(PAR)$ is described in Zhang et al. (2002a) and is not repeated here. The dimensionless functions $f(T)$, $f(D)$ and $f(\Psi)$ represent the conductance-reducing effects of air temperature T, water-vapour-pressure deficit D, and water stress (leaf water potential) Ψ, respectively, on leaf stomatal conductance (Brook et al., 1999a). The equations for these functions are:

$$f(T) = \frac{T - T_{\min}}{T_{\mathrm{opt}} - T_{\min}}\left[\frac{T_{\max} - T}{T_{\max} - T_{\mathrm{opt}}}\right]^{b_t} \tag{6a}$$

with

$$b_t = \frac{T_{\max} - T_{\mathrm{opt}}}{T_{\max} - T_{\min}} \tag{6b}$$

$$f(D) = 1 - b_{\mathrm{vpd}}D \tag{6c}$$

with

$$D = e^*(T) - e \tag{6d}$$

and

$$f(\Psi) = (\Psi - \Psi_{c2})/(\Psi_{c1} - \Psi_{c2}) \tag{6e}$$

with

$$\Psi = -0.72 - 0.0013\mathrm{SR}. \tag{6f}$$

T_{min} and T_{max} are minimum and maximum temperatures (° C) that indicate the temperatures below and above which complete stomatal closure occurs. T_{opt} is an optimum temperature that indicates the temperature of maximum stomatal opening. b_{vpd} is a water-vapour-pressure-deficit constant (kPa^{-1}), D is the vapour pressure deficit (kPa), $e^*(T)$ is the saturation water vapour pressure (kPa) at air temperature T (° C), and e is the ambient water vapour pressure (kPa). Ψ_{c1} and Ψ_{c2} (MPa) are parameters that specify leaf-water-potential dependency. When $\Psi > \Psi_{\mathrm{c1}}$ (i.e. no leaf water potential stress), $f(\Psi) = 1.0$. Values for all parameters required for calculating R_{st} are taken from Brook et al. (1999a), Dorman and Sellers (1989), Dickinson et al. (1986), and NOAA (1992) library data, and are listed in Table 1. These parameters are r_{smin} (minimum stomatal resistance), b_{rs} (empirical constant in stomatal resistance), T_{min}, T_{max}, T_{opt}, b_{vpd}, Ψ_{c1} and Ψ_{c2}.

During nighttime when there is no solar radiation, the leaf stomata are assumed to be completely closed. R_{st} estimated from Eq. (2) then has an infinite value. Recent research suggests that the stomata of some canopy species may still be partially open even at night (Gunthardt-Goerg et al., 1997; Musselman and Minnick, 2000; Wiser and Havranek, 1993, 1995). However, this behaviour is difficult to quantify given present knowledge. In this study we treat the stomata as fully closed at night.

$\mathbf{R_{ac}}$: In-canopy aerodynamic resistance should be the same for all gaseous species. The equation developed in Zhang et al. (2002b) is used:

$$R_{ac} = \frac{R_{ac0} LAI^{1/4}}{u_*^2}, \tag{7}$$

where LAI is the leaf area index, u_* is the friction velocity, and R_{ac0} is the reference value for in-canopy aerodynamic resistance. R_{ac0} is expected to vary with different canopies and suggested values are given in Table 1 for all LUC. For some LUC, a range of R_{ac0} values are given to reflect the change of canopy structure at different times in the growing season. The minimum values, $R_{ac0}(\text{min})$, correspond to leafless periods for deciduous forests and earlier growing periods for agricultural lands. The maximum values, $R_{ac0}(\text{max})$, correspond to the full-leaf period for forests and the maturity period for agricultural lands. Here a simple equation is suggested for extracting R_{ac0} values for any day of the year based on minimum and maximum LAI values since this information is available in most air-quality models:

$$R_{\mathrm{ac0}}(t) = R_{\mathrm{ac0}}(\mathrm{min}) = \frac{LAI(t) - LAI(\mathrm{min})}{LAI(\mathrm{max}) - LAI(\mathrm{min})}\left[R_{\mathrm{ac0}}(\mathrm{max}) - R_{\mathrm{ac0}}(\mathrm{min})\right], \tag{7a}$$

where $R_{\mathrm{ac0}}(t)$ corresponds to the R_{ac0} value at any day of the year. $LAI(\mathrm{min})$ and $LAI(\mathrm{max})$ represents minimum and maximum LAI values, respectively, during the year.

$\mathbf{R_g}$: Surface resistance is considered separately for different surface types (water, ice, snow, soil). The following equaiton is used according to Erisman et al. (1994):

$$R_g = \begin{cases} R_{\mathrm{water}} \\ R_{\mathrm{ice}} \\ R_{\mathrm{snow}} \\ R_{\mathrm{soil}} \end{cases}, \tag{8}$$

where R_{water}, R_{ice}, R_{snow} and R_{soil} represent resistance to water, ice, snow, and soil surfaces, respectively. R_{snow} and R_{ice} are assumed to have the same values. For O_3, R_{water}, R_{snow} and R_{ice} are given a value of $2000\,\mathrm{s\,m^{-1}}$. For SO_2, R_{water} is given a value of $20\,\mathrm{s\,m^{-1}}$, while R_{snow} and R_{ice} are taken as a function of temperature with a lower limit of $100\,\mathrm{s\,m^{-1}}$ and an upper limit of $500\,\mathrm{s\,m^{-1}}$ (Erisman et al., 1994) as follows:

$$R_{\mathrm{snow}}, R_{\mathrm{ice}}(\mathrm{SO_2}) = 70(2 - T). \tag{8a}$$

Information on R_{soil} is limited for both O_3 and SO_2, as discussed in Zhang et al. (2002b). Based on previous studies, a value of $200\,\mathrm{s\,m^{-1}}$ is given for O_3 for all vegetated surfaces (LUC 4-19, 25 and 26) and $500\,\mathrm{s\,m^{-1}}$ for non-vegetated surfaces or

© EGU 2003

surfaces with wet ground (LUC 20-24). R_{soil} is more complicated for SO_2 due to its sensitivity to wetness. Thus, soil resistance to SO_2 may be smaller when dew or rain occurs. The following approach is suggested for R_{soil} for SO_2:

$$R_{\mathrm{soil}} = \begin{cases} R_{\mathrm{gd}} \\ R_{\mathrm{grain}} \\ R_{\mathrm{gdew}} \end{cases}, \tag{8b}$$

where R_{gd} represents the soil resistance over land surfaces with no dew or rain has occurred, R_{grain} and R_{gdew} are the resistances to soil when rain or dew occur. Values of 50 and 100 s m^{-1} are assigned to R_{grain} and R_{gdew}, respectively. Suggested R_{gd} values for all LUCs are presented in Table 1. For canopies with relatively high soil moisture content (e.g. tropical forest), R_{gd} is given a smaller value compared to vegetation types with dry soils (e.g. desert).

A more rigorous approach for R_{soil} is to separate soil into dry and wet portions (Zhang et al., 2002a). However, the information on the wet fraction of soil is usually not available. Although a sophisticated method for extracting this fraction is available (Sellers et al., 1996), this method requires more detailed information than is typically available in air-quality models.

R$_{\mathrm{cut}}$: Canopy cuticle resistance is calculated for dry and wet conditions separately according to Zhang et al. (2002b):

$$R_{\mathrm{cutd}} = \frac{R_{\mathrm{cutd0}}}{e^{3\mathrm{RH}} LAI^{1/4} u_*} \tag{9a}$$

$$R_{\mathrm{cutw}} = \frac{R_{\mathrm{cutw0}}}{LAI^{1/2} u_*}, \tag{9b}$$

where RH is relative humidity (as a fraction). R_{cutd0} and R_{cutw0} are reference values for dry and wet cuticle resistance, respectively. When rain or dew occurs, the canopy is treated as wet. Values of R_{cutd0} and R_{cutw0} for O_3 and values of R_{cutd0} for SO_2 for

© EGU 2003

each LUC are presented in Table 1. R_{cutw0} for SO_2 is treated differently under dew and rain conditions. For all vegetated surfaces values of $50\,\mathrm{s\,m^{-1}}$ and $100\,\mathrm{s\,m^{-1}}$ are given for R_{cutw0} for rain and dew conditions, respectively. Equations (9a) and (9b) were developed based on the 5-site flux data set for which $u*$ values seldom exceeded $1.5\,\mathrm{m\,s^{-1}}$ for the two forest locations and $0.8\,\mathrm{m\,s^{-1}}$ for the other three sites (crops). It is expected that these equations give reasonable values for most conditions, but they may give unrealistically small values for SO_2 when $u*$ is extremely large (e.g. $u* > 2\,\mathrm{m\,s^{-1}}$). Thus, a lower limit of $100\,\mathrm{s\,m^{-1}}$ is suggested for dry canopies and $20\,\mathrm{s\,m^{-1}}$ for wet canopies for SO_2.

In winter when temperatures are below -1° C, R_{gd} and R_{cutd} are increased by as much as double their original value according to the equation:

$$R_{\mathrm{gd}}(T < -1^\circ \mathrm{C}) = R_{\mathrm{gd}} e^{0.2(-1-T)} \tag{10a}$$

$$R_{\mathrm{cutd}}(T < -1^\circ \mathrm{C}) = R_{\mathrm{cutd}} e^{0.2(-1-T)}. \tag{10b}$$

For snow on the ground and leaves, both R_g and R_{cut} are adjusted by including a snow cover fraction (f_{snow}):

$$\frac{1}{R_g} = \frac{1-2f_{\mathrm{snow}}}{R_g} + \frac{2f_{\mathrm{snow}}}{R_{\mathrm{snow}}} \tag{10c}$$

$$\frac{1}{R_{\mathrm{cut}}} = \frac{1-f_{\mathrm{snow}}}{R_{\mathrm{cut}}} + \frac{f_{\mathrm{snow}}}{R_{\mathrm{snow}}}. \tag{10d}$$

Since snow on ground persists longer than on leaves for high canopies, the snow fraction for the ground (R_g) is taken as 2 times that of leaves (R_{cut}). Note that both f_{snow} and $2f_{\mathrm{snow}}$ have a range of values between 0.0-1.0. Since the snow fraction is usually not available from meteorological models, a simple equation is suggested to estimate

f_{snow} from snow depth (SD in cm):

$$f_{\mathrm{snow}} = \frac{sd}{sd_{\max}}, \tag{10e}$$

where $sd_{\max}$ is a parameter at or above which value the snow fraction for canopy leaves is assumed to be 1. Suggested $sd_{\max}$ values are also listed in Table 1 (Note that the actual $sd_{\max}$ for underlying soil surfaces is only half of the values presented in Table 1 as can be seen from the comparison of Eqs. 10c and 10d).

3. Other parameters

LAI is an extremely important parameter for calculating canopy resistances. LAI values used in GEM are adopted here. Monthly LAI values at the beginning of each month are presented in Fig. 2. LAI values on any day are interpolated using the day number of the month. Note that several LUC that have constant LAI values are not shown in Fig. 2. They are set to 5.0 (LUC 4), 6.0 (LUC 5, 8), 4.0 (LUC 9, 23), 3.0 (LUC 10, 12) and 0.0 (LUC 1-3, 22, 24). LAI values for LUC 21 (urban) are set to a constant value of 1 in GEM. Since LAI values for urban locations in different regions can have quite different seasonal variations, here we choose to give LAI a value of 0.1 in the winter season, gradually increasing to 1 in the late spring. We keep it as 1 until early fall, and then reduce it gradually to 0.1 again at the end of fall (figure not shown).

Roughness length (z_0) is needed for calculating friction velocity, which subsequently affects aerodynamic resistance and non-stomatal resistance. z_0 from GEM cannot be used directly since it is treated together with topography. Suggested z_0 values for each LUC are presented in Table 1. For water surfaces (LUC 1 and 3), z_0 is calculated as a function of wind speed. For some surfaces a constant z_0 value is suggested, while for others a range of z_0 values is given. For those surfaces that have variable z_0 values, an equation similar to Eq. (7a) is used to obtain z_0 for any time period based on LAI

© EGU 2003

values:

$$z_o(t) = z_0(\min) + \frac{LAI(t) - LAI(\min)}{LAI(\max) - LAI(\min)} \left[z_0(\max) - z_0(\min)\right] . \tag{11}$$

Note that for higher canopies and canopies with large LAI, z_0 is given a larger value.

4. Model evaluation and example output

The non-stomatal resistance parameterization has been evaluated in Zhang et al. (2002b, 2003) using O_3 and SO_2 flux data from 5 sites. Here measurements of O_3 and SO_2 dry deposition data at one site (deciduous forest in Pennsylvania, USA) are used to show the performance of the revised model. This site is chosen because it has a large data set for O_3 and SO_2 under both dry and wet canopy conditions (Finkelstein et al., 2000). The other 4 sites have very few SO_2 measurements over wet canopies. Figure 3 shows the observed mean diurnal cycle of half-hourly V_d along with the modelled estimates. The suitability of the current model can be seen from the very good agreement of O_3 deposition over wet canopies (Fig. 3b) and SO_2 deposition over both dry and wet canopies (Figs. 3c and 3d). As discussed in Zhang et al. (2002b), earlier models could not predict the diurnal cycle of O_3 and SO_2 V_d over wet canopies since meteorological conditions are not explicitly considered. Although the non-stomatal resistance parameterization was developed based on O_3 flux data, it also gives very good results for SO_2 over dry and wet canopies with adjustments of species-dependent parameters (Table 1), and the results for SO_2 from the current model compare better to the data than do earlier models (Finkelstein et al., 2000; Zhang et al., 2002a). It is noted that there is an underestimation of O_3 V_d during mid-morning hours when maximum V_d appeared. This problem also exists in other models since most models predict maximum V_d around noon. Since the daytime O_3 V_d is mainly controlled by stomatal uptake, adopting the new non-stomatal resistance parameterization will not solve the problem shown in Fig. 3a. It is worth pointing out that the phenomenon of mid- morning maximum V_d has only been observed over several forest canopies and not over crops (Finkelstein et al., 2000). More research is needed on this phenomenon before model improvements can be made.

Based upon the model structure described above we expect model results to be sensitive to several of the input parameters, namely LAI, z_0, $u*$, SR, T and RH. These parameters can vary widely due to meteorological variations (i.e., hourly to daily) and seasonal variation, as well as geographic variations. Due to this large variation, it is difficult to provide typical V_d values from the model. We therefore ran the model for a wide but realistic range of input values for these parameters, and estimated the typical range of V_d values that can be expected. Here we present the results for each LUC under dry canopy conditions assuming a reference height for the V_d calculation of 20 m. The range of $u*$ values used depended upon LUC with the two roughest surfaces, evergreen broadleaf forests (LUC 5 and 8), being assumed values within the range of 0.1–1.5 m s^{-1}; forests and urban areas, a range of 0.1–1.2 m s^{-1}; and the remaining surfaces, a range of 0.1–0.8 m s^{-1}. Surface temperature was allowed to vary between −10 and 30° C, solar radiation from 0 to 800 W m^{-2} and relative humidity from 50–90%. All possible contributions of $u*$, T, SR and RH were input separately into the model (using small increments for all variables: 0.1 for $u*$, 1° C for T, 50 Wm^{-2} for SR and 5% for RH) to calculate the range of V_d values possible for each LUC. In addition, calculations were done for the first day of every month so that the seasonal variation in LAI was accounted for. Since, realistically, some of the test conditions would be highly unlikely (e.g. high temperatures and large solar radiation over tundra), the allowed ranges were adjusted so that 5oC is the minimum temperature for tropical forests and 20° C and 500 W m^{-2} are the maximum values for tundra. Although information (i.e. scaling parameters) on a total of 30 species is available in Zhang et al. (2002a), we show results for only 9 species in Table 2. Overall, we expect that the maximum V_d values extracted from these model test runs will be representative of the real-world typical maximum V_d for most land types under dry conditions.

The model test results in Table 2 indicate that maximum V_d values occur when LAI

Title Page
Abstract Introduction
Conclusions References
Tables Figures
◀◀ ▶▶
◀ ▶
Back Close
Full Screen / Esc
Print Version
Interactive Discussion

© EGU 2003

is large, the temperature is close to an optimum value (Topt in Table 1), $u*$ is large, RH is high and solar radiation is relatively strong (not necessarily maximum SR for some canopies due to the water stress, see Eq. 6). The maximum V_d values for forest canopies and agricultural lands range around 1.1–1.7 cm s^{-1} for SO_2, 1.0–1.4 cm s^{-1} for O_3, and 3.5–5.1 cm s^{-1} for HNO_3. NO_2 V_d follows the pattern of O_3 V_d but with slightly smaller values ($\alpha = 0$, $\beta = 0.8$). H_2O_2 V_d is higher than both SO_2 and O_3 during both day and night ($\alpha = 1$, $\beta = 1$). HNO_3 has the highest V_d among all the chemical species considered here due to its high solubility and reactivity ($\alpha = 10$, $\beta = 10$). The V_d of PAN mimics the pattern of O_3 ($\alpha = 0$, $\beta = 0.6$) but is always smaller while the V_d of HCHO follows the pattern of SO_2 ($\alpha = 0.8$, $\beta = 0.2$). NH_3 is similar to SO_2 ($\alpha = 1$, $\beta = 0$), but slightly higher during the day due to its higher molecular diffusivity. The V_d of ROOH is similar to V_d of O_3 ($\alpha = 0.1$, $\beta = 0.8$). Zhang et al. (2002a) reviewed and discussed all published measurements for all species of interest. Most flux measurements of SO_2, O_3, NO_2, NH_3 and HNO_3 support the results generated from the present model. The very limited set of measurements for PAN, HCHO, H_2O_2 and ROOH also agree well with model results. There are no data for many of the species presented in Zhang et al. (2002a) and thus the present model provides a tool to estimate their deposition rates.

To attempt to provide an indication of the typical V_d values (instead of maximum range as shown in Table 2) and to demonstrate the effect of day vs. night, wet vs. dry and snow, we ran the model again and used typical values for the input parameters. Figure 4 shows the $u*$ values used for different LUCs for several typical conditions. Note that $u*$ for dry and wet summer days was given the same set of values. Typically LUC 5 (evergreen broadleaf trees) and 8 (tropical broadleaf trees) can expect to have the largest $u*$ values reflecting their large roughness; conversely, smooth surfaces (ice, water, tundra) have the smallest $u*$ values. The other dominant meteorological variables used for the tests are: 20° C (T), 75% (RH) and 600 Wm^{-2} (SR) for dry summer day; 20° C (T) and 200 Wm^{-2} (SR) for rain summer day; 10° C (T) and 75% (RH) for dry summer night; and –2° C (T) and 20 cm (SD) for snow condition (note that for ice surfaces, the temperature is given a value of -2° C for all the tests).

For SO_2 and O_3, V_d is found to typically be around 0.6–1.0 cm s^{-1} for a summer day for most vegetated surfaces with dry canopy conditions. As expected, V_d is larger over canopies with larger LAI and smaller r_{smin}. Stomatal resistance is the dominant term during dry daytime conditions. When canopies are wet due to rain, SO_2 V_d increases substantially for vegetated surfaces while O_3 V_d increases only slightly. During nighttime over dry canopies, SO_2 V_d is around 0.2–0.4 cm s^{-1}, and O_3 V_d is 0.1–0.3 cm s^{-1}. V_d of SO_2 is larger than that of O_3 due to the smaller cuticle and soil resistances assigned to SO_2. Note that during nighttime over wet canopies caused by rain (figure not presented), V_d of O_3 is slightly larger compared to dry nighttime conditions, while V_d of SO_2 can be substantially larger. When canopies are wetted by dew, both SO_2 and O_3 have slightly larger V_d values compared to dry nighttime conditions. In winter when there is snow, SO_2 V_d is around 0.4 cm s^{-1}. However, it can be close to 1 cm s^{-1} over snow surfaces if the temperature is higher than 1° C (see Eq. 8a). O_3 V_d is less than 0.1 cm s^{-1} if the surfaces are fully covered by snow, but can be higher than 0.2 if the surfaces are partially covered by snow (e.g. forest canopies).

It is well known that surface resistance for HNO_3 is very small. Thus, aerodynamic resistance usually dominates the rate of HNO_3 dry deposition. Figure 5 shows that for summer daytime dry canopy conditions, V_d of HNO_3 is higher than 1.5 cm s^{-1} for canopies with small roughness lengths and as high as 3 cm s^{-1} for forest canopies with larger roughness lengths. Under wet conditions, V_d values are even larger. During nighttime, HNO_3 V_d is still close to 1.0 cm s^{-1} for canopies with small z_0 values and even higher for canopies with large z_0. As discussed earlier, and also shown in Fig. 5, V_d of HCHO follows the pattern of SO_2 and V_d of PAN mimics the pattern of O_3. Overall, the typical V_d values shown in Fig. 5 are consistent with the published measurements reviewed by Sehmel (1984), Brook et al. (1999b), Wesely and Hicks (2000) and Zhang et al (2002a).

5. Conclusions

A parameterization for estimating dry deposition velocities in air-quality models is revised by including a newly developed non-stomatal resistance formulation, a realistic treatment of cuticle and ground resistance in winter (low temperature, snow surfaces) and the handling of seasonally-dependent input parameters (i.e. LAI, z_0, resistance components). Evaluation using measurement data demonstrates that this model predicts more accurate deposition velocities compared to other existing models, especially for wet canopies. Model produced maximum deposition velocities and values for typical meteorological conditions are realistic compared to published measurements.

There are few measurements of V_d for species other than SO_2, O_3, NO_2, HNO_3, NH_3. So, although the approach presented here and in Zhang et al. (2002a) are expected to be reasonably realistic, the estimated values are unvalidated due to the lack of data. Further developments will rely on the availability of more detailed measurements in the future. Furthermore, it is recommended that future field campaigns include direct flux measurements of different gases so the scaling method can be validated, and at several levels inside canopies, e.g. at the canopy floor so that soil resistance can be estimated. Separate measurements of stomatal and non-stomatal uptake is also important for evaluating the model and for estimating O_3 damage to crops.

Acknowledgement. We express our appreciation of S. Belair and J. St-James of the Canadian Meteorological Center in Montreal for providing GEM related information. We are also grateful to M. D. Moran of the Meteorological Service of Canada for his very helpful comments.

References

Baldocchi, D. D.: A multi-layer model for estimating sulfur dioxide deposition to a deciduous oak forest canopy, Atmos. Environ., 22, 869–884, 1988.

Baldocchi, D. D., Hicks, B. B., and Camara, P.: A canopy stomatal resistance model for gaseous deposition to vegetated surfaces, Atmos. Environ., 21, 91–101, 1987.

Brook, J., Zhang, L., Franco, D., and Padro, J.: Description and evaluation of a model of deposition velocities for routine estimates of air pollutant dry deposition over North America, Part I: Model development, Atmos. Environ., 33, 5037–5052, 1999a.

Brook, J., Zhang, L., Franco, D., and Padro, J.: Description and evaluation of a model of deposition velocities for routine estimates of air pollutant dry deposition over North America, Part II: Review of past measurements and model results, Atmos. Enviro., 33, 5053–5070, 1999b.

Byun, D. W., and Ching, J. K. S.: Science Algorithms of the EPA Models-3 Community Multiscale Air Quality (CMAQ) Modeling System, EPA/600/R-99/030, Environmental Protection Agency, Office of Research and Development, Washington, DC, 1999.

Carmichael, G. R., Peters, L. K., and Saylor, R. D.: The STEM-II regional scale acid deposition and photochemical oxidant model, 1: An overview of model development and applications, Atmos. Environ., 25, 2077–2090, 1991.

Chang, J. S., Brost, R. A., Isaksen, I. S. A., Madronich, S., Middleton, P., Stockwell, W. R., and Walcek, C. J.: A three-dimensional Eulerian acid deposition model: Physical concepts and formulation, J. Geophys. Res., 92, 14681–14700, 1987.

Coté, J., Desmarais, J. G., Gravel, S., Methot, A., Patoine, A., Roch, M., and Staniforth A.: The operational CMC/MRB global environmental multiscale (GEM) model, Part I, design considerations and formulation, Mon. Wea. Rev., 126, 1373–1395, 1997.

Dickinson, R. E., Henderson-Sellers, A., Kennedy, P. J., and Wilson, M. F.: Biosphere-Atmosphere Transfer Scheme (BATS) for the NCAR Community Climate Model. NCAR Technical Note NCAR/TN275+STR, National Centre for Atmospheric Research, Boulder, Colorado, 67, 1986.

Dorman, J. L. and Sellers, P. J.: A global climatology of albedo, roughness length and stomatal resistance for atmospheric general circulation models as represented by the simple biosphere model (SiB), J. Appl. Meteor, 28, 833–855, 1989.

Erisman, J. W., Van Pul, A., and Wyers, P.: Parameterization of surface resistance for the quantification of atmospheric deposition of acidifying pollutants and ozone, Atmos. Environ., 28, 2595–2607, 1994.

Finkelstein, P. L., Ellestad, T. G., Clarke, J. F., Meyers, T. P., Schwede, D., Hebert, E. O. and Neal, J. F.: Ozone and sulfur dioxide dry deposition to forests: observations and model evaluation, J. Geophy. Res., 105, 15 365–15 377, 2000.

Gunthardt-Goerg, M. S., Mcquattie, C. J., Scheidegger, C., Rhiner, C., and Matyssek, R.:

Ozone-induced cytochemical and ultrastructrual changes in leaf mesophyll cell walls, Canadian Journal of Forest Research, 27, 453–463, 1997.

Harley, R. A., Russell, A. G., McRae G. J., Cass, G. R., and Seinfeld, J. H.: Photochemical modeling of the Southern California Air Quality Study, Environ. Sci. Tech., 27, 378–388, 1993.

Hicks, B. B., Baldocchi, D. D., Meyers, T. P., Hosker, R. P. Jr., and Matt, D. R.: A preliminary multiple resistance routine for deriving dry deposition velocities from measured quantities, Water, Air, and Soil Pollution, 36, 311–330, 1987.

Janssen, L. H. J. M. and Romer, F. G.: The frequency and duration of dew occurrence over a year, Tellus, 43B, 408–419, 1991.

Jarvis, P. G.: The interpretation of the variations in leaf water potential and stomatal conductance found in canopies in the field, Phil. Trans. R. Soc. London Ser. B, 273, 593–610, 1976.

Lamaud, E., Carrara, A., Brunet, Y., Lopez, A., and Druilhet, A.: Ozone fluxes above and within a pine forest canopy in dry and wet conditions, Atmos. Environ., 36, 77–88, 2002.

Laville, P., Cellier, P., Lamaud, E., and Lopez. A.: Micrometeorological measurements of ozone fluxes on a maize crop during the ESCOMPTE experiment, Presented at Joint International Symposium on Atmospheric Chemistry within the Earth System, 18–25 September 2002, Crete, Greece, Abstract and Poster, 2002.

Lopez, A., Bouchou, P., Brustet, J. M., and Fontian, J.: Ozone vertical fluxes at the interface vegetation-atmosphere, Presented at Joint International Symposium on Atmospheric Chemistry within the Earth System, 18–25 September 2002, Crete, Greece, Abstract and Poster, 2002.

Meyers, T. P., Finkelstein, P. L., Clarke, J., Ellestad, T. G., and Sims, P. F.: A multi-layer model for inferring dry deposition using standard meteorological measurements, J. Geophy. Res., 103, D17, 22 645–22 661, 1998.

Moran, M. D., Dastoor, A., Gong, S. L., Gong, W., and Makar, P. A.: Proposed conceptual design for the AES regional particulate-matter model/unified model, Unpublished report, Meteorological Service of Canada, Downsview, Ontario, Canada, 100 (available from first author), 1998.

Musselman, R. C. and Minnick, T. J.: Nocturnal stomatal conductance and ambient air quality standards for ozone, Atmos. Environ., 34, 719–733, 2000.

NOAA: NOAA library of input data for “Bigleaf” and “Multi-layer” models, ATDD, NOAA, Oak Ridge, TN, 1992.

Padro, J.: Summary of ozone dry deposition velocity measurements and model estimates over vineyard, cotton, grass and deciduous forest in summer, Atmos. Environ., 30, 2363–2369, 1996.

Padro, J., den Hartog, G., and Neumann, H. H.: An investigation of the ADOM dry deposition module using summertime O_3 measurements above a deciduous forest, Atmos. Environ., 25, 1689–1704, 1991.

Pleim, J. E. and Xiu, A.: Development and testing of a surface flux and planetary boundary layer model for application in mesoscale models, J. Appl. Meteor., 34, 16–32, 1995.

Pudykiewicz, J. A., Kallaur, A., and Smolarkiewicz, P. K.: Semi-Lagrangian modelling of tropospheric ozone, Tellus, 49B, 231–248, 1997.

Sehmel, G. A.: Deposition and resuspension, In Atmospheric science and power production, Edited by Randerson, D. 533–583, NTIS, Springfield, VA, 1984.

Scire, J. S.: A review of the UAM-V dry deposition algorithm and recommendations for dry deposition modeling in the LMOS study region, Sigma Research Corporation, Westford, MA (Document A195-100), 1991.

Sellers, P. J., Randall, D. A., Collatz, J. G., Berry, J. A., Field, C. B., Dazlich, D. A., Collelo, G. D., and Bounoua, L.: A revised land surface parameterization (SiB2) for atmospheric GCMs, Part I: Model formulation, J. of Climate, 9, 676–705, 1996.

Smith, R. I., Fowler, D., Sutton, M. A., Flechard, C., and Coyle, M.: Regional estimation of pollutant gas dry deposition in the UK: Model description, sensitivity analyses and outputs, Atmos. Environ., 34, 3757–3777, 2000.

Wesely, M. L.: Parameterization of surface resistances to gaseous dry deposition in regional-scale numerical models, Atmos. Environ., 23, 1293–1304, 1989.

Wesely, M. L. and Hicks, B. B.: A review of the current status of knowledge in dry deposition, Atmos. Environ., 34, 2261–2282.

Wiser, G. and Havranek, W. M.: Ozone uptake in the sun and shade crown of spruce: quantifying the physiological effects of ozone exposure, Trees, 7, 227–232, 1993.

Wiser, G. and Havranek, W. M.: Environmental control of ozone uptake in Larix decidua Mill: a comparison between different altitudes, Tree Physiology, 15, 253–258, 1995.

Zhang, L., Moran, M., Makar, P., Brook, J., and Gong, S.: Modelling Gaseous Dry Deposition in AURAMS A Unified Regional Air-quality Modelling System, Atmos. Environ., 36, 537–560, 2002a.

Zhang, L., Brook, J., and Vet, R.: On Ozone dry deposition – With emphasis on non-stomatal uptake and wet canopies, Atmos. Environ., 36, 4787–4799, 2002b.

Zhang, L., Brook, J., and Vet, R.: Evaluation of a non-stomatal resistance parameterization for SO_2 dry deposition, Atmos. Environ., 37, in press, 2003.

© EGU 2003

Table 1. Land use categories and all related parameters (na = not applicable; f(u) means a function of wind speed)

LUC		R_{ac0}	R_{cutd0} O_3	R_{cutdw} O_3	R_{cutd0} SO_2	R_{gd} SO_2	r_{stmin} ($s\ m^{-1}$)	b_{rs} (Wm^{-2})	T_{min} (°C)	T_{max} (°C)	T_{opt} (°C)	b_{vpd} (kPa^{-1})	ψ_{c1} (Mpa)	ψ_{c2} (MPa)	z_0 (m)	Sdmax (cm)
1	water	0	na	na	na	20	na	na	na	na	na	na	na	na	f(u)	na
2	ice	0	na	na	na	Eq.8a	na	na	na	na	na	na	na	na	0.01	1
3	inland lake	0	na	na	na	20	na	na	na	na	na	na	na	na	f(u)	na
4	evergreen needleleaf trees	100	4000	200	2000	200	250	44	-5	40	15	0.31	-2	-2.5	0.9	200
5	evergreen broadleaf trees	250	6000	400	2500	100	150	40	0	45	30	0.27	-1	-5.0	2.0	400
6	deciduous needleleaf trees	60-100	4000	200	2000	200	250	44	-5	40	15	0.31	-2	-2.5	0.4-0.9	200
7	deciduous broadleaf trees	100-250	6000	400	2500	200	150	43	0	45	27	0.36	-1.9	-2.5	0.4-1.0	200
8	tropical broadleaf trees	300	6000	400	2500	100	150	40	0	45	30	0.27	-1	-5.0	2.5	400
9	drought deciduous trees	100	8000	400	6000	300	250	44	0	45	25	0.31	-1	-4.0	0.6	200
10	evergreen broadleaf shrubs	60	6000	400	2000	200	150	40	0	45	30	0.27	-2	-4.0	0.2	50
11	deciduous shrubs	20-60	5000	300	2000	200	150	44	-5	40	15	0.27	-2	-4.0	0.05-0.2	50
12	thorn shrubs	40	5000	300	2000	200	250	44	0	45	25	0.27	-2	-3.5	0.2	50
13	short grass and forbs	20	4000	200	1000	200	150	50	5	40	30	0	-1.5	-2.5	0.04	5
14	long grass	10-40	4000	200	1000	200	100	20	5	45	25	0	-1.5	-2.5	0.02-0.1	20
15	crops	10-40	4000	200	1500	200	120	40	5	45	27	0	-1.5	-2.5	0.02-0.1	10
16	rice	10-40	4000	200	1500	50	120	40	5	45	27	0	-1.5	-2.5	0.02-0.1	10
17	sugar	10-40	4000	200	2000	200	120	50	5	45	25	0	-1.5	-2.5	0.02-0.1	10
18	maize	10-50	5000	300	2000	200	250	65	5	45	25	0	-1.5	-2.5	0.02-0.1	10
19	cotton	10-40	5000	300	2000	200	125	65	10	45	30	0	-1.5	-2.5	0.02-0.2	10
20	irrigated crops	20	4000	200	2000	50	150	40	5	45	25	0	-1.5	-2.5	0.05	10
21	urban	40	6000	400	4000	300	200	42	0	45	22	0.31	-1.5	-3	1.0	50
22	tundra	0	8000	400	2000	300	150	25	-5	40	20	0.24	0	-1.5	0.03	2
23	swamp	20	5000	300	1500	50	150	40	0	45	20	0.27	-1.5	-2.5	0.1	10
24	Desert	0	na	na	na	700	na	na	na	na	na	na	na	na	0.04	2
25	mixed wood forests	100	4000	200	2500	200	150	44	-3	42	21	0.34	-2	-2.5	0.6-0.9	200
26	Transitional forest	100	4000	200	2500	200	150	43	0	45	25	0.31	-2	-3	0.6-0.9	200

© EGU 2003

© EGU 2003

Table 2. Range of deposition velocities (in cm s^{-1}) for 9 chemical species over all land types under dry canopy conditions

LUC		SO_2	O_3	NO_2	H_2O_2	HNO_3	PAN	HCHO	NH_3	ROOH
1	water	0.118 - 2.07	0.036 - 0.05	0.030 - 0.04	0.119 - 2.13	0.119 - 2.61	0.024 - 0.03	0.119 - 1.93	0.121 - 2.18	0.099 - 0.47
2	ice	0.129 - 0.80	0.038 - 0.05	0.032 - 0.04	0.132 - 0.85	0.146 - 2.91	0.025 - 0.03	0.128 - 0.68	0.133 - 0.82	0.073 - 0.14
3	inland lake	0.118 - 2.07	0.036 - 0.05	0.030 - 0.04	0.119 - 2.13	0.119 - 2.61	0.024 - 0.03	0.119 - 1.93	0.121 - 2.18	0.099 - 0.47
4	evergreen needleleaf trees	0.025 - 1.51	0.017 - 1.19	0.015 - 1.09	0.033 - 2.09	0.114 - 5.07	0.013 - 0.80	0.024 - 1.60	0.026 - 1.83	0.017 - 1.18
5	evergreen broadleaf trees	0.020 - 1.67	0.010 - 1.23	0.009 - 1.15	0.026 - 2.17	0.106 - 5.33	0.007 - 0.83	0.018 - 1.78	0.020 - 2.07	0.011 - 1.24
6	deciduous needleleaf trees	0.025 - 1.51	0.017 - 1.19	0.015 - 1.09	0.031 - 2.09	0.081 - 5.07	0.013 - 0.80	0.024 - 1.60	0.025 - 1.83	0.017 - 1.18
7	deciduous broadleaf trees	0.018 - 1.44	0.010 - 1.16	0.009 - 1.10	0.022 - 1.89	0.068 - 5.07	0.007 - 0.79	0.017 - 1.59	0.018 - 1.88	0.010 - 1.16
8	tropical broadleaf trees	0.079 - 1.64	0.039 - 1.21	0.033 - 1.13	0.107 - 2.13	0.166 - 5.33	0.027 - 0.82	0.072 - 1.75	0.080 - 2.04	0.041 - 1.22
9	drought deciduous trees	0.013 - 0.92	0.012 - 0.83	0.011 - 0.75	0.018 - 1.23	0.074 - 3.97	0.010 - 0.56	0.013 - 0.90	0.014 - 1.00	0.012 - 0.79
10	evergreen broadleaf shrub	0.027 - 1.15	0.017 - 0.94	0.016 - 0.90	0.032 - 1.48	0.102 - 3.49	0.015 - 0.65	0.025 - 1.26	0.028 - 1.47	0.018 - 0.94
11	deciduous shrubs	0.027 - 1.18	0.018 - 1.01	0.017 - 0.96	0.033 - 1.54	0.094 - 3.53	0.015 - 0.70	0.026 - 1.31	0.028 - 1.53	0.019 - 1.01
12	thorn shrubs	0.031 - 1.04	0.023 - 0.83	0.021 - 0.76	0.037 - 1.39	0.105 - 3.56	0.019 - 0.56	0.030 - 1.10	0.031 - 1.25	0.023 - 0.82
13	short grass and forbs	0.049 - 1.18	0.038 - 0.80	0.036 - 0.72	0.055 - 1.54	0.114 - 3.20	0.033 - 0.54	0.048 - 1.19	0.050 - 1.35	0.038 - 0.80
14	long grass	0.041 - 1.58	0.025 - 1.26	0.023 - 1.21	0.047 - 1.96	0.112 - 3.43	0.021 - 0.88	0.039 - 1.72	0.042 - 2.00	0.026 - 1.27
15	crops	0.035 - 1.49	0.024 - 1.28	0.022 - 1.23	0.042 - 1.90	0.104 - 3.43	0.020 - 0.90	0.034 - 1.66	0.036 - 1.92	0.024 - 1.28
16	rice	0.037 - 1.74	0.024 - 1.36	0.022 - 1.31	0.044 - 2.08	0.104 - 3.43	0.019 - 0.96	0.035 - 1.90	0.037 - 2.18	0.024 - 1.40
17	sugar	0.031 - 1.37	0.024 - 1.26	0.022 - 1.21	0.039 - 1.80	0.099 - 3.43	0.020 - 0.89	0.030 - 1.56	0.032 - 1.80	0.024 - 1.25
18	maize	0.029 - 1.03	0.020 - 0.81	0.018 - 0.75	0.035 - 1.36	0.097 - 3.41	0.017 - 0.56	0.027 - 1.08	0.029 - 1.24	0.020 - 0.80
19	cotton	0.031 - 1.31	0.022 - 1.14	0.021 - 1.08	0.038 - 1.71	0.098 - 3.63	0.019 - 0.79	0.030 - 1.46	0.032 - 1.70	0.022 - 1.13
20	irrigated crops	0.045 - 1.39	0.033 - 0.64	0.030 - 0.58	0.049 - 1.61	0.100 - 3.22	0.027 - 0.42	0.044 - 1.38	0.046 - 1.56	0.036 - 0.74
21	urban	0.025 - 0.76	0.022 - 0.58	0.021 - 0.51	0.030 - 1.13	0.069 - 4.44	0.019 - 0.37	0.025 - 0.79	0.026 - 0.89	0.022 - 0.57
22	tundra	0.051 - 0.97	0.039 - 0.53	0.036 - 0.48	0.057 - 1.12	0.103 - 3.07	0.031 - 0.35	0.050 - 0.92	0.052 - 1.04	0.039 - 0.55
23	swamp	0.045 - 1.70	0.029 - 0.96	0.027 - 0.91	0.050 - 1.97	0.114 - 3.43	0.024 - 0.65	0.043 - 1.76	0.046 - 2.02	0.032 - 1.06
24	Desert	0.049 - 0.75	0.061 - 0.19	0.053 - 0.16	0.082 - 0.87	0.142 - 2.27	0.043 - 0.12	0.052 - 0.66	0.050 - 0.77	0.056 - 0.24
25	mixed wood forests	0.021 - 1.56	0.016 - 1.42	0.015 - 1.33	0.028 - 2.19	0.103 - 5.07	0.013 - 0.96	0.020 - 1.75	0.021 - 2.03	0.016 - 1.39
26	Transitional forest	0.021 - 1.55	0.016 - 1.41	0.015 - 1.32	0.028 - 2.19	0.103 - 5.07	0.013 - 0.95	0.020 - 1.74	0.021 - 2.02	0.016 - 1.38

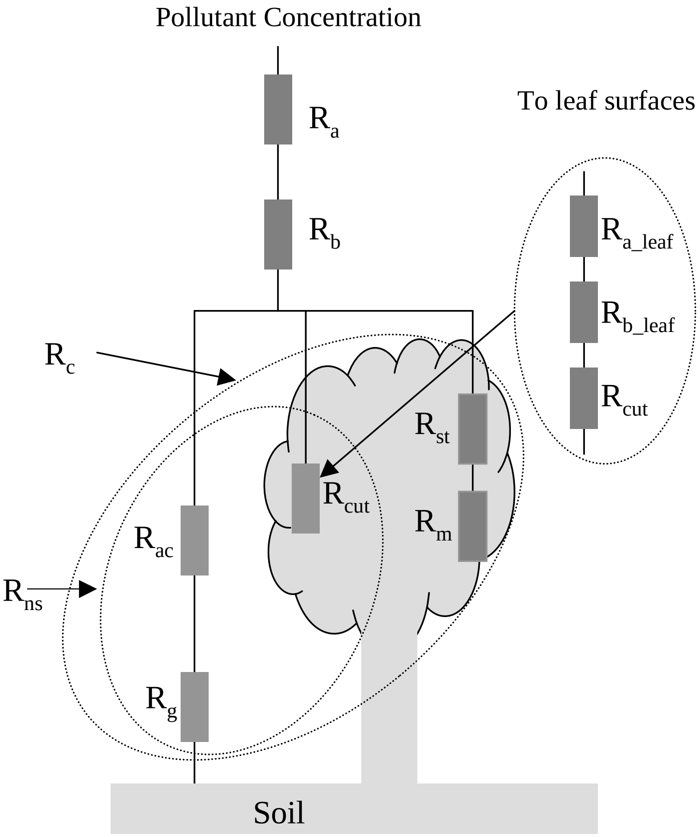

Fig. 1. Scheme of resistance analogy.

Title Page
Abstract | Introduction
Conclusions | References
Tables | Figures
◀| |▶
◀ ▶
Back | Close
Full Screen / Esc
Print Version
Interactive Discussion

© EGU 2003

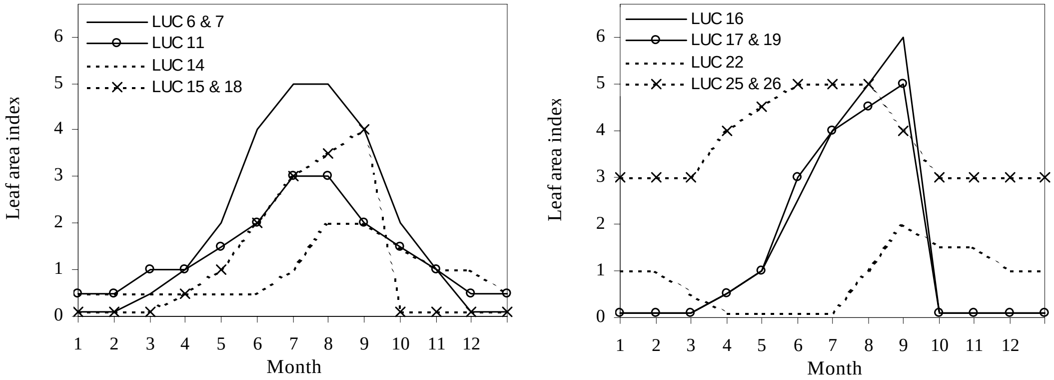

Fig. 2. Leaf area index in the Northern Hemisphere.

Title Page
Abstract
Introduction
Conclusions
References
Tables
Figures
◀◀
▶▶
◀
▶
Back
Close
Full Screen / Esc
Print Version
Interactive Discussion

© EGU 2003

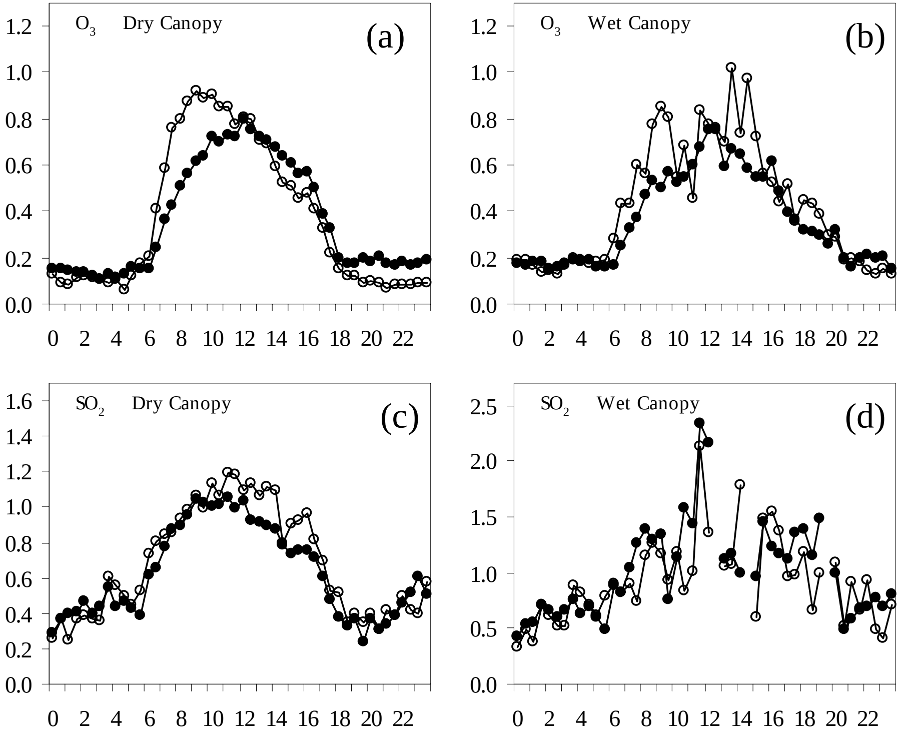

Fig. 3. Average diurnal cycle of modelled (filled points) and observed (open points) deposition velocities.

Title Page
Abstract
Introduction
Conclusions
References
Tables
Figures
◀◀
▶▶
◀
▶
Back
Close
Full Screen / Esc
Print Version
Interactive Discussion

© EGU 2003

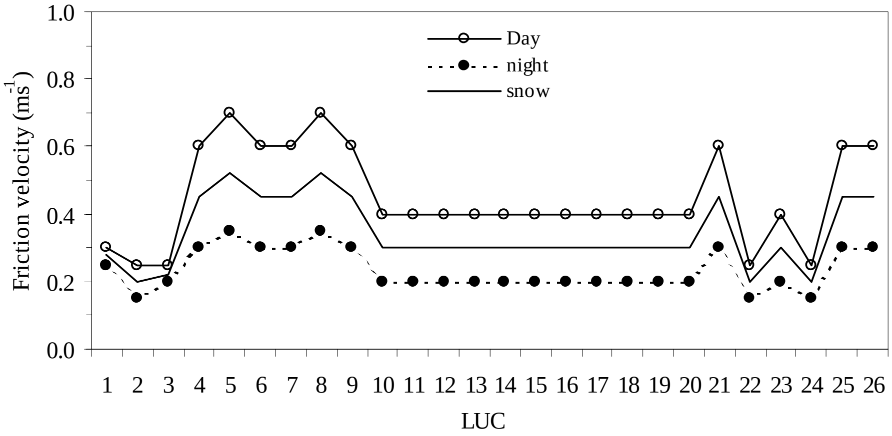

Fig. 4. Friction velocity values used for producing Fig. 5.

© EGU 2003

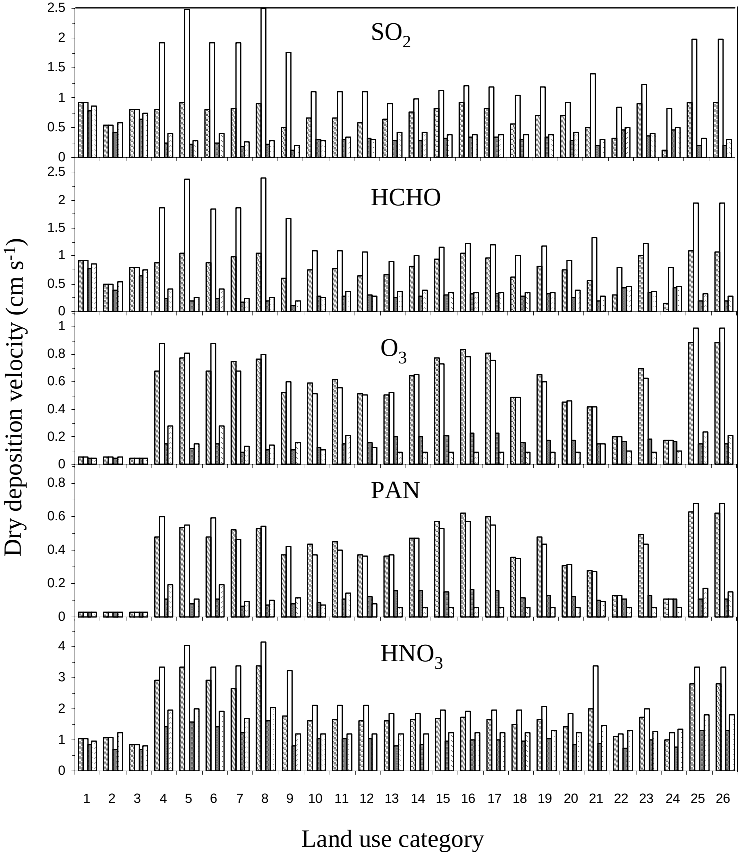

Fig. 5. Dry deposition velocity for chemical species SO$_2$, HCHO, O$_3$, PAN and HNO$_3$ under 4 typical conditions: dry summer day, rain summer day, dry summer night and winter with snow (shown, respectively as 4 columns from left to right).

© EGU 2003